Supplementary Table 1: Crystallographic statistics

Data collection and processing statistics		
Space Group	C2221	
Unit cell dimensions a, b, c (Å) α, β, γ (^{0})	 100.73, 300.75, 182.09 90.0, 90.0, 90.0	
Resolution (Å)	46.19 – 4.50 (4.74 - 4.50)*	
Mosaicity (^{0})	0.2	
Reflections (total/unique)	122385/16854	
Mean I/σ(I)	12.9 (2.4)	
Completeness	99.8 (99.8)	
R_{merge}(%)	9.5 (85.2)	
Multiplicity	7.3(7.4)	
Refinement statistics		
	model 1	model 2
Resolution (Å)	4.50	4.50
R_{work}/R_{free} (%)	33.9/39.7	45.0/47.0
RMSD bond length (Å)	0.007	0.008
RMSD bond angle (°)	0.990	1.4
# non-hydrogen protein atoms	4767	4785
# non-hydrogen DNA atoms	2971	3091

* Values in parentheses are for highest-resolution shell

Supplementary Table 2: Nucleosome binding data using nucleosomes labeled at two different positions (H4 Q27C and H4 G56C)

	K_d(H4 Q27C)	vs wt	K_d(H4 G56C)	vs wt
Set8Δ1	7.9 ± 0.6 nM	**1.0**	16.5 ± 3.9 nM	**1.0**
Set8Δ1(R179A,K180A	20 ± 2 nM	**2.6**	54 ± 26 nM	**3.3**
Set8Δ1(R188A,R188A)	2500 ± 400 nM	**320**	5600 ± 2900 nM	**340**
Set8Δ1(K256A,K257A,R258A, K341A,H347F)	330 ± 50 nM	**42**	81 ± 24 nM	**4.9**

Supplementary Figures

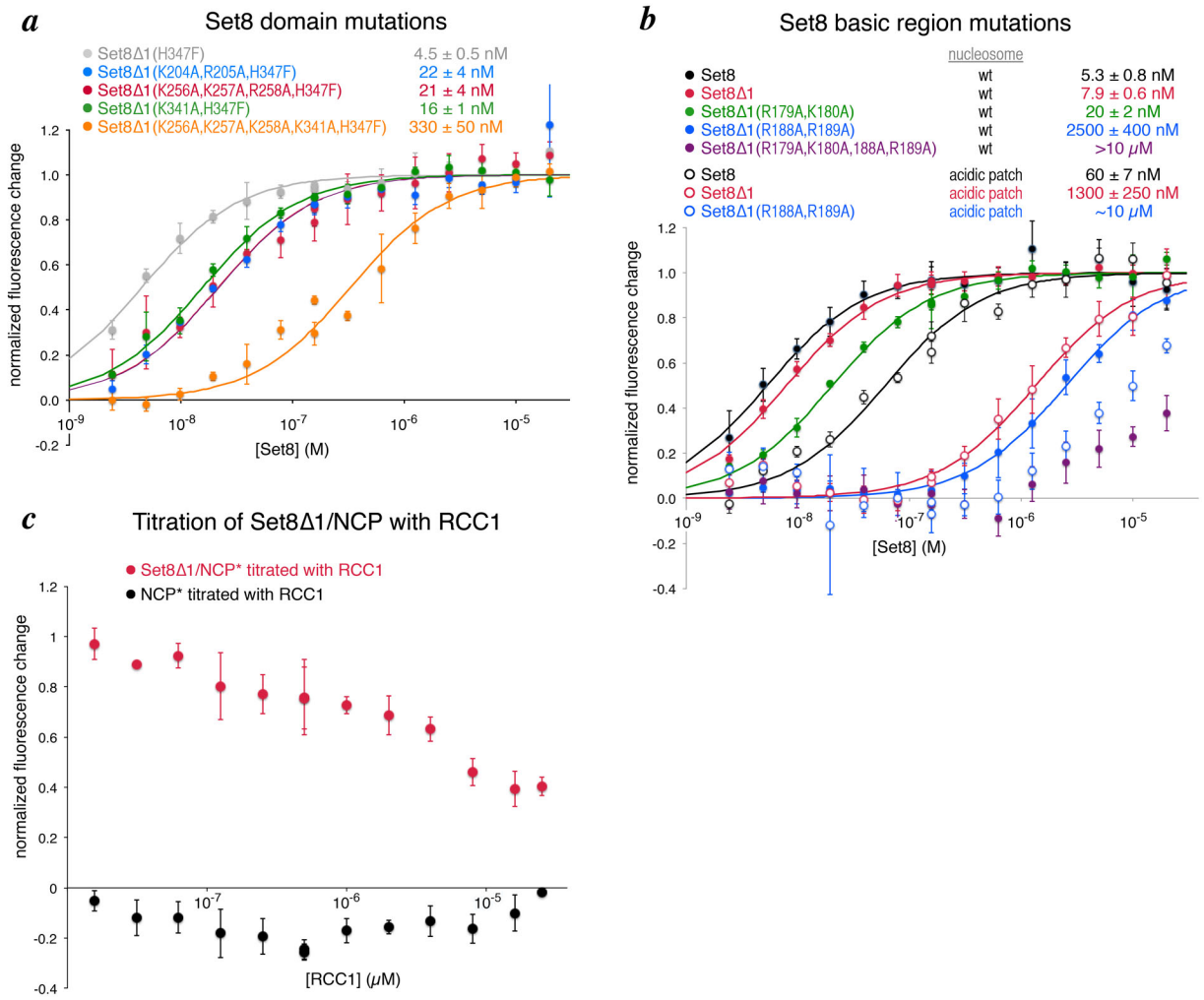

Suppl. Fig. 1: Nucleosome binding data for (a) Set8 domain mutations, (b) Set8 basic region mutations, and (c) titration of Set8/nucleosome with RCC1.
(a) and (b) Nucleosome fluorescently labeled with Oregon Green 488 on H4Q27C were titrated with Set8 variants in triplicate, and the normalized fluorescence change plotted as a function of Set8 concentration. The calculated dissociation constants are shown above the binding curves. (c) Nucleosome binding data for Set8Δ1/nucleosome or nucleosome titrated with RCC1 show RCC1 can partially compete with Set8Δ1 for binding to nucleosomes.

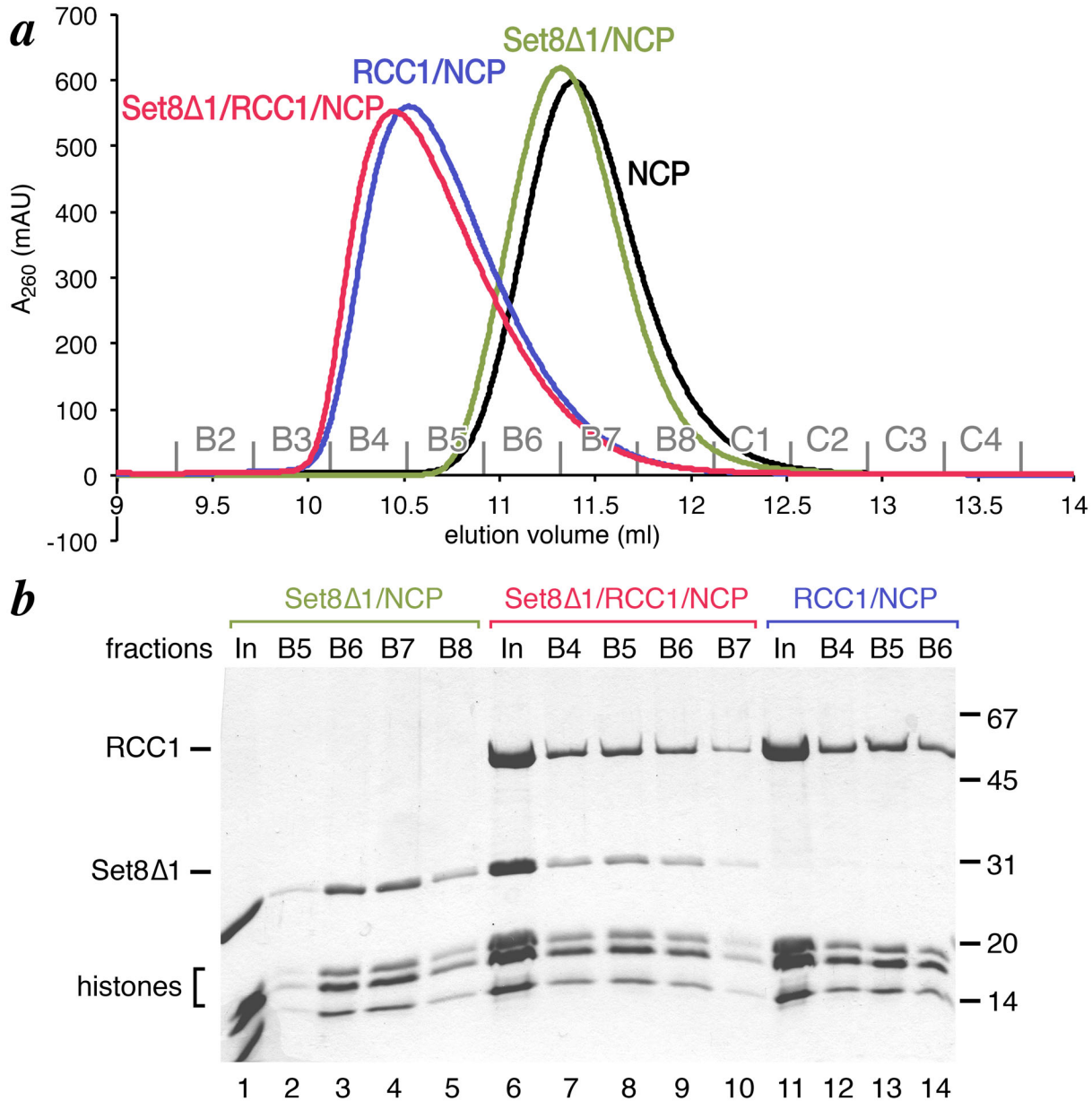

Suppl. Fig. 2: Set8, RCC1 and the nucleosome core particle (NCP) can form a ternary complex.
(a) The Set8/RCC1/NCP (red), RCC1/NCP (blue), Set8/NCP (green) and NCP only (black) samples were separated over a Superdex 200 HR size exclusion chromatography column. The elution fractions and times are shown above and below the x-axis respectively. (b) SDS-PAGE gel of select fractions from the chromatography runs shown in part (a). Molecular weights of standards are shown on the right.

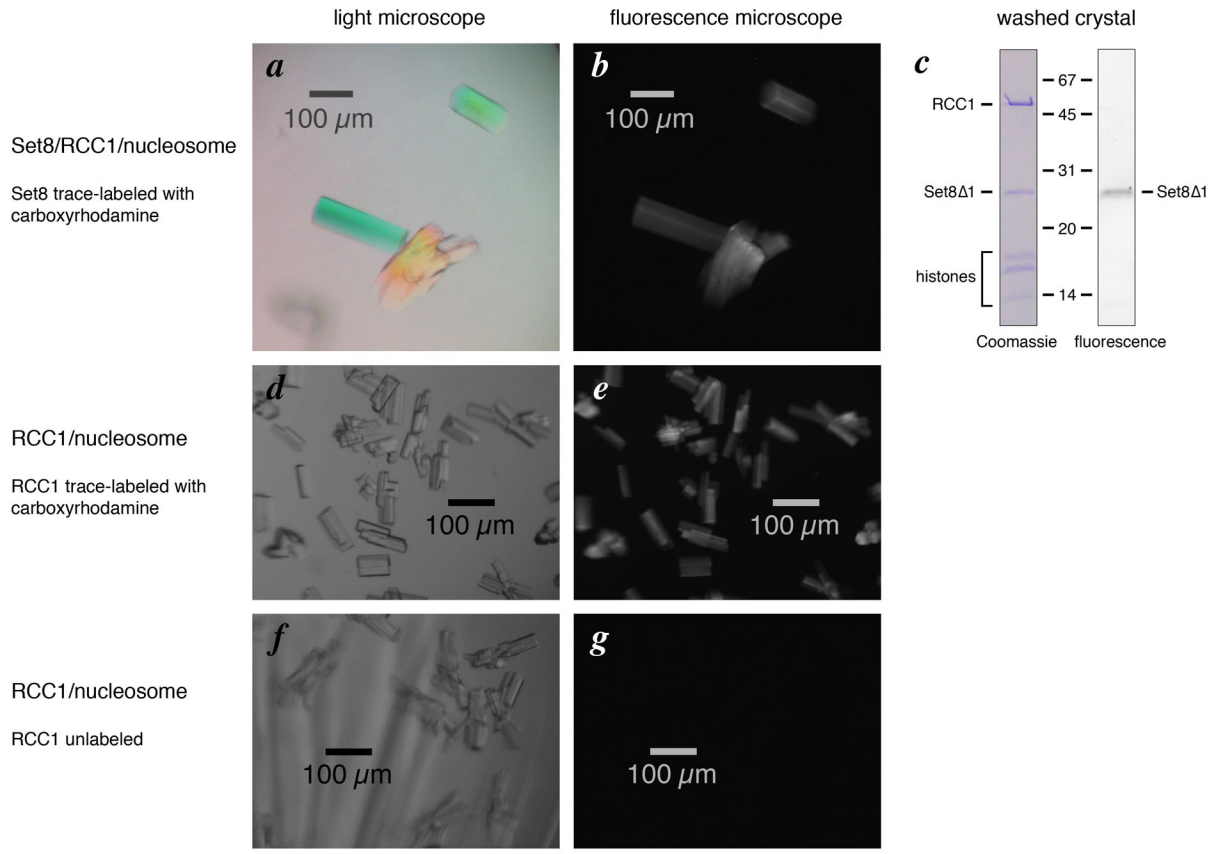

Suppl. Fig. 3: Analysis of Set8/RCC1/nucleosome crystals.
(a) and (b) Crystals in Set8/RCC1/nucleosome trials visualized by (a) light microscopy or (b) fluorescence microscopy. The Set8 protein was trace-labeled with carboxyrhodamine red, (c) Washed Set8/RCC1/nucleosome crystal analyzed by Coomassie staining (left) and fluorescence (right).
(d) and (e) Positive control showing RCC1/nucleosome crystals grown using RCC1 trace-labeled with carboxyrhodamine, visualized by (d) light microscopy or (e) fluorescence microscopy. Similar unlabeled crystals were used to determine the crystal structure of the RCC1/nucleosome complex (refs. 28 & 29)
(f) and (g) Negative control showing RCC1/nucleosome crystals grown using unlabeled RCC1, visualized by (f) light microscopy or (g) fluorescence microscopy.

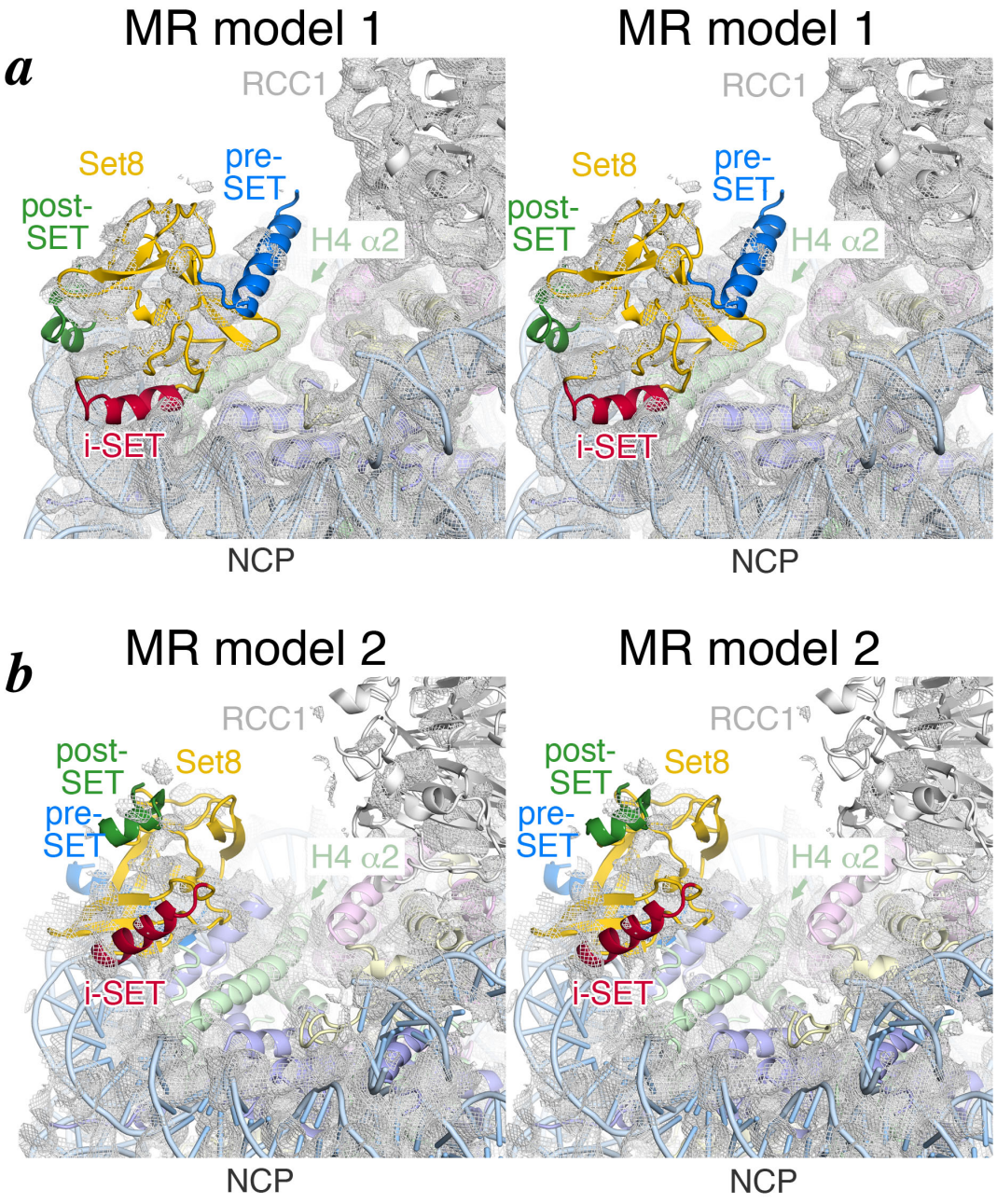

Suppl. Fig. 4: Stereo $2F_o$-F_c electron density maps for Set8/RCC1/nucleosome molecular replacement (MR) models 1 and 2 contoured at 1 σ cutoff.
(a) In MR model 1, clear and continuous electron density is visible for RCC1 and for the histone polypeptide backbone and DNA components of the nucleosome, including histone H4 α2 helix, but poor and discontinuous density was observed for Set8 including the pre-SET, i-SET and post-SET regions. (b) In MR model 2, discontinuous density is visible for RCC1 and the nucleosome, and even poorer discontinuous density is visible for Set8. In contrast to model 1, the electron density for the histone H4 α2 helix is not vislble at this contour.